

# Longitudinal phase-space matching between radio-frequency systems with different harmonic numbers and accelerating voltages

V. Ziemann, FREIA, Uppsala University

December 19, 2021

## Abstract

We describe a simple mechanism to transform bunches with matched longitudinal phase-space distributions from one RF system to a matched distribution of a second RF system operating on a different harmonic and with a different accelerating voltage. The process is reversible and the longitudinal emittance is preserved. Simple equations that characterize the procedure are given and applications are discussed. In particular this method can be used to rapidly shorten the bunch length in proton rings.

## 1 Introduction

Handing over a beam from one RF system to a second one operating at a different frequency and voltage frequently occurs when transferring beams from one ring to another or to manipulate the bunch length in order to satisfy experimental requirements. Of course it is desirable that the beam quality is preserved in these transitions, in particular, the phase-space area occupied by the beam—the longitudinal emittance—should remain unchanged. To analyze this scenario we consider a beam, controlled by one radio-frequency (RF) system, operating with harmonic number  $h_1$  and voltage  $V_1$  to a second system, operating with harmonic  $h_2$  and voltage  $V_2$ . The dynamics of particles in a RF system—or in the longitudinal phase space of a storage ring—is described by

$$\ddot{\phi} + \Omega_s^2 \sin \phi = 0 \quad \text{with} \quad \Omega_s^2 = -\frac{\omega_{\text{rf}} \eta \cos \phi_s}{\beta^2 T_0} \frac{e \hat{V}}{E_0} \quad (1)$$

with the synchrotron frequency  $f_s = \Omega_s/2\pi$ , the RF frequency  $f_{\text{rf}} = \omega_{\text{rf}}/2\pi$  and voltage  $\hat{V}$ , the phase slip factor  $\eta$ , the design phase  $\phi_s$ , the speed of the protons  $\beta = v/c$ , the beam energy  $E_0$ , and the revolution time  $T_0$ . We assume that we operate under conditions where  $\eta \cos \phi_s < 0$  such that the stable phase is at

$\phi = 0$ . We will always use  $\Omega_s$  at the first harmonic and voltage  $\hat{V}$  as reference and note that the synchrotron tune  $\Omega(v, h)$  at voltage  $v\hat{V}$  and harmonic  $h$  is related to  $\Omega_s$  by  $\Omega(v, h) = \sqrt{vh}\Omega_s$ . Henceforth we will always use the lower-case relative voltages in this report.

For the transitions we take inspiration from the 'bunch-muncher' described in [1], which was used to shorten the bunches extracted from the damping rings of the SLAC linear collider by briefly reducing the RF voltage and then turning it back on to rotate the bunch in longitudinal phase space. To analyze this scenario and to derive equations that govern the transitions we employ a linearized theory in the following section.

## 2 Linear theory

If we can assume that the bunches are short compared to the wavelength of the RF systems the dynamics of the particles is governed by the linearized equation  $\ddot{\phi} + \Omega_s^2\phi = 0$  and their motion can be described by the transfer matrix

$$\hat{R}(t) = \begin{pmatrix} \cos(\Omega_s t) & \sin(\Omega_s t)/\Omega_s \\ -\Omega_s \sin(\Omega_s t) & \cos(\Omega_s t) \end{pmatrix}. \quad (2)$$

that operates on the state of  $(\phi, d\phi/dt)$ . If we consider motion at another harmonic number  $h$  and voltage  $v$ , we need to adapt the matrix to

$$\begin{aligned} R(h, v, t) &= \begin{pmatrix} 1/h & 0 \\ 0 & 1 \end{pmatrix} \begin{pmatrix} \cos(\Omega t) & \sin(\Omega t)/\Omega \\ -\Omega \sin(\Omega t) & \cos(\Omega t) \end{pmatrix} \begin{pmatrix} h & 0 \\ 0 & 1 \end{pmatrix} \\ &= \begin{pmatrix} \cos(\sqrt{vh}\Omega_s t) & \sin(\sqrt{vh}\Omega_s t)/\sqrt{vh^3}\Omega_s \\ -\sqrt{vh^3}\Omega_s \sin(\sqrt{vh}\Omega_s t) & \cos(\sqrt{vh}\Omega_s t) \end{pmatrix}, \quad (3) \end{aligned}$$

where we use the abbreviation  $\Omega = \sqrt{vh}\Omega_s$ . The two outer matrices in the first equality are necessary to scale the phase at harmonic  $h$ , because there are  $h$  buckets in the longitudinal extent where there is only one bucket at the first harmonic. Essentially we stretch the phase-axis first, then we rotate, and finally we transform back into the phase space of the first harmonic.

It is now straightforward to verify that a matched beam  $\sigma(v, h)$  is proportional to

$$\sigma(h, v) = \begin{pmatrix} 1/\sqrt{vh^3}\Omega_s & 0 \\ 0 & \sqrt{vh^3}\Omega_s \end{pmatrix}. \quad (4)$$

It reproduces after transport with  $R(v, h, t)$  from Equation 3, such that it obeys  $\sigma(h, v) = R\sigma(h, v)R^\top$ .

Our task is now to find a transfer matrix  $M$  that transforms one matched beam with parameters  $h_1$  and  $v_1$  to another one with  $h_2$  and  $v_2$ , or  $\sigma(h_2, v_2) = M\sigma(v_1, h_1)M^\top$ . In the 'bunch-muncher' from [1] the voltage  $v_1$  of the first RF

State	$h$	$v$	Duration
Initially in first system	$h_1$	$v_1$	arbitrary
First part of transfer	$h_1$	$\hat{v} = v_1 \sqrt{\frac{v_1}{v_2}} \left(\frac{h_1}{h_2}\right)^{3/2}$	$t_1 = \pi / \left(2\sqrt{\hat{v}h_1}\Omega_s\right)$
Second part of transfer	$h_1$	$v_1$	$t_2 = \pi / \left(2\sqrt{v_1h_1}\Omega_s\right)$
Finally in second system	$h_2$	$v_2$	arbitrary

Table 1: The parameters for a transition from on RF system to another one.

system is lowered to  $\hat{v}$  for some time  $t_1$  and later restored to its original value  $v_1$ , which results in a shortened bunch. If we now realize that choosing the time  $t$  to obey  $\sqrt{vh}\Omega_s t = \pi/2$  the transfer matrix  $R$  becomes

$$S(h, v) = \begin{pmatrix} 0 & 1/\sqrt{vh^3}\Omega_s \\ -\sqrt{vh^3}\Omega_s & 0 \end{pmatrix}. \quad (5)$$

We now build our transforming system from two such matrices, one with a reduced voltage  $\hat{v}$  and duration  $t_1 = \pi / \left(2\sqrt{\hat{v}h_1}\Omega_s\right)$  and a second one with restored voltage  $v_1$  and duration  $t_2 = \pi / \left(2\sqrt{v_1h_1}\Omega_s\right)$ . The transfer matrix  $M$  for the transition, which we will call a *munch*, is then given by

$$M = S(h_1, v_1)S(h_1, \hat{v}) = \begin{pmatrix} -\sqrt{\hat{v}/v_1} & 0 \\ 0 & -\sqrt{v_1/\hat{v}} \end{pmatrix}. \quad (6)$$

The condition for  $\sigma(h_2, v_2) = M\sigma(h_1, v_1)M^\top$  to be valid then leads to the condition

$$\sqrt{v_2h_2^3}\Omega_s = \frac{v_1}{\hat{v}}\sqrt{v_1h_1^3}\Omega_s \quad \text{or} \quad \frac{\hat{v}}{v_1} = \sqrt{\frac{v_1}{v_2}} \left(\frac{h_1}{h_2}\right)^{3/2}, \quad (7)$$

which gives us the voltage during the munch  $\hat{v}$  that is needed to transform the matched longitudinal phase space of the first RF system to that of the second system. This condition and the respective durations are summarized in Table 1.

In passing we note that the matrix  $M$  is diagonal, but at the same time, is defined as the product of two off-diagonal matrices from Equation 5. This resembles the construction of the (transverse) transfer matrix for a telescope that is based on two modules, each consisting of a thin lens with focal length  $f$ , sandwiched between drift spaces of length  $f$ . Such a module has zeros on the diagonal and  $f$  and  $-1/f$  on the off-diagonal. Two such modules with focal length  $f_1$  and  $f_2$  then produce the matrix for the telescope that has  $-f_1/f_2$  and its inverse on the diagonal. We note that in Equation 5 the term  $1/\sqrt{vh^3}\Omega_s$  takes the role of the focal length  $f$ . The bunch-muncher can thus be understood as a telescope in longitudinal phase space.

The bunch length  $\tilde{\sigma}_i = \sqrt{\sigma(h_i, v_i)}$  changes from one step to the next by the magnification  $|M_{11}|$  from Equation 6, such that we obtain

$$\frac{\tilde{\sigma}_2}{\tilde{\sigma}_1} = \sqrt{\frac{\hat{v}}{v_1}} = \left(\frac{v_1}{v_2}\right)^{1/4} \left(\frac{h_1}{h_2}\right)^{3/4}. \quad (8)$$

We now need to see whether the linearized theory also works if we use the dynamics of the non-linear system of the mathematical pendulum from Equation 1.

### 3 Model

During the transitions only one RF system operates at a time, such that the dynamics of the protons in longitudinal phase-space is governed by Equation 1, which describes the phase space of this mathematical pendulum and also synchrotron oscillations. A characteristic feature of the dynamics is the existence of a separatrix, given for the first harmonic by the equation

$$\dot{\phi} = \pm 2\Omega_s \cos(\phi/2). \quad (9)$$

This separatrix separates the periodic from the unbounded phase-space trajectories. Moreover, closed-form solutions of the equations of motion for the pendulum equation, expressed in terms of Jacobi-elliptic functions [2], are available [3]. Using these solutions makes step-by-step integration obsolete, but only work if the design phase  $\phi_s$  is zero and only if one RF system is operational at a time. These conditions apply in our case and we therefore adapt the MATLAB [4] software that accompanies [3] to handle different harmonics  $h$  and voltages  $v$ .

## 4 Simulations

Here we consider several transitions from one RF system to another, where we always use the bunch-munch equations from Table 1, but use the closed-form solution of the pendulum equation to follow a large number of sample particles.

### 4.1 Voltage step

In the first simulation we consider a transition from a first-harmonic system when increasing the voltage by a factor of five, where we follow 10000 particles of a matched initial distribution that has an rms bunch length of  $10^\circ$ .

The left-hand image in Figure 1 shows the evolution of the harmonic number in the upper and of the voltage in the lower panel. We see that the harmonic does not change from its initial value  $h = 1$ , but the voltage changes during the munch. First it is reduced and subsequently restored to its previous value, which is visible prior to increasing the voltage to five times its initial value.

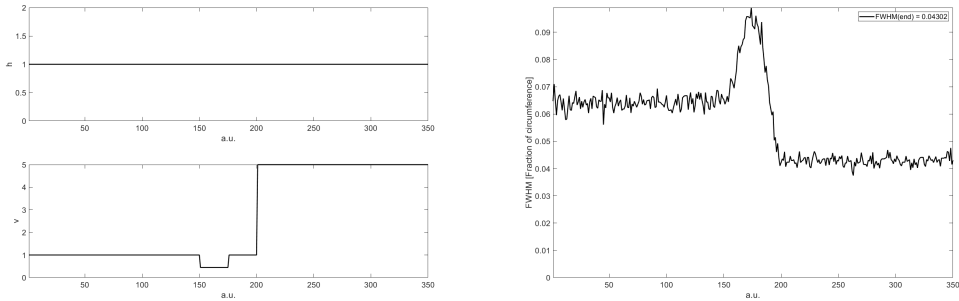


Figure 1: The evolution of the harmonic (top left), the voltage (bottom left) and the bunch length (right) for the matched voltage step.

The image on the right-hand side shows the full-width at half maximum (FWHM) of the distribution along the horizontal axis—the bunch length. Note that we normalize it to the circumference of the ring. We see that the FWHM is initially constant, where the displayed time corresponds to 1.5 synchrotron-oscillation periods. Then the FWHM increases as a consequence of the dropped voltage during the bunch and then decreases to the smaller value, required to obtain a matched distribution at the five times increased voltage. Then the FWHM does not significantly change any more, indicating that the distribution is indeed a matched one. The reduction of the FWHM to about 70 % of its initial value is consistent with the value  $(v_1/v_2)^{1/4} = (1/5)^{1/4} \approx 0.67$  from Equation 8.

## 4.2 Sequence of harmonics

In the following simulation we transfer the distribution from the first to the third and on to the eleventh harmonic and then transfer back through similar intermediate stages to the initial configuration.

We start with a matched distribution of 10000 particles with an rms bunch length of  $10^\circ$  of the first-harmonic RF system, which is shown on the left plot in the first row in Figure 2. Note that the horizontal axis shows the phase  $\phi$ , at the first harmonic such that the shown axis corresponds to the circumference of the ring. The vertical axis shows  $d\phi/dt$  and the black line shows the separatrix. Note that the maximum height of the separatrix corresponds to the momentum acceptance of the RF system.

Then we create a number of transitions, where we transfer from the first harmonic to the third and then to the eleventh harmonic, before returning back via the third to the first harmonic. In detail the steps are given in Table 2, where the first column refers to the position in Figure 2, the second and third give the harmonic  $h$  and voltage  $v$ , whereas the last column contains a description of the state. In Figure 2 we show the bunch distribution at the end of each state

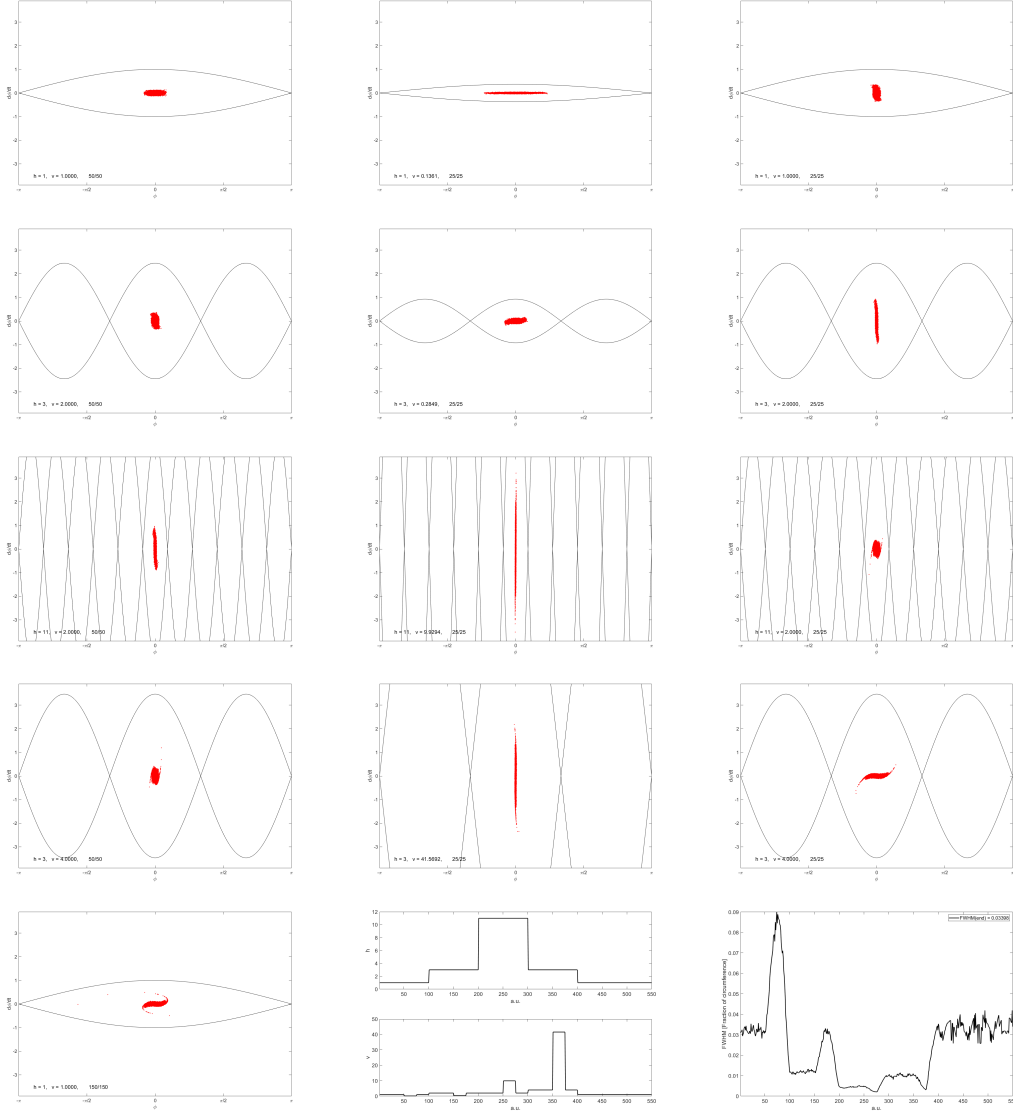


Figure 2: The phase-space distributions for the  $h = 1, 3, 11, 3, 1$  sequence of harmonics. In the top row shows the bunch to prepare the distribution for the third harmonic. The second row shows the bunch for the eleventh harmonic, followed by the bunch back to the third and first harmonic in the third and fourth row. The middle plot in the bottom row shows the evolution of harmonic (upper) and voltage (lower) and the plot on the right shows the evolution of the bunch length.

Row, Column	Harmonic $h$	Voltage $v$	Comment
1,1	1	1	Initial distribution
1,2	1	0.136	Munch to $h = 2, v = 3$
1,3	1	1	
2,1	3	2	Third harmonic
2,2	3	0.285	Munch to $h = 11, v = 2$
2,3	3	2	
3,1	11	2	Eleventh harmonic
3,2	11	9.93	Munch back to $h = 3, v = 4$
3,3	11	2	
4,1	3	4	Third harmonic
4,2	3	42.57	Munch back to $h = 1, v = 1$
4,3	3	4	
5,1	1	1	Back at the first harmonic

Table 2: The steps in the second simulation though the sequence of harmonics.

described in Table 2. In the first row the three images show the initial distribution on the left, the distribution at the end of the munch and on the right after the quarter-period rotation with the restored voltage. At this point the bunch is still governed by the first harmonic, but already has the shape of the matched distribution of the third harmonic. At this point we turn off the first-harmonic system, turn on the third-harmonic system, and follow the distribution for half a synchrotron period. It is shown on the first image in the second row, which is practically the same distribution as the one we handed over to the third. At this point we lower the voltage of the third harmonic—the second munch—and show the stretched distribution on the image in the middle of the second row, followed by the distribution after the quarter oscillation with restored voltage, shown on the right. At this point the distribution is matched to the eleventh harmonic and we turn off the third harmonic and turn on the eleventh. The distribution after half a synchrotron oscillation is shown on the left image in the third row.

At this point we decide to reverse the sequence. In the first stage we have to munch back to the third harmonic and that entails to briefly, albeit significantly, increase the RF voltage of the eleventh, which is shown in the middle image in the third row. Subsequently restoring the voltage to the original value for a quarter period turns the distribution to a matched distribution suitable for the third harmonic (at a different voltage than before). After turning off the eleventh-harmonic system and turning on the third we show the distribution after half a synchrotron period in the first image in the fourth row. Next we increase the voltage, shown in the middle image, and after a quarter oscillation with restored voltage the distribution is suitable for the first harmonic, shown on the right. Turning off the third harmonic and turning on the first, we follow the

distribution for 1.5 synchrotron periods after which it is shown on the left image in the bottom row. It looks very similar to the original distribution on the top-left image, only some spiral arms have developed because in some intermediate state, particles moved outside the linear regime of the pendulum equation. The upper panel on the image in the middle of the bottom row shows the evolution of the harmonic  $h$  as the simulation progressed and the lower panel shows the voltage  $v$ . Here we note that in particular the voltage during the step-down sequence reaches prohibitively large values, which are likely to be impossible in a real machine. That the simulation nevertheless shows that the method works can be seen from the image on the bottom right in Figure 2. It shows the FWHM of the distribution—the bunch length. We find that the final FWHM is only slightly larger and more noisy than the initial value. We attribute the noisiness to the spiral arms of the final distributions. Note also that the munches where the bunch is lengthened show up as spikes on the plot and that the smallest values of the FWHM are below one percent of the circumference. For a 300 m ring this is in the tens of ns range.

We can draw a number of conclusions. First, the steps preserve the longitudinal phase-space area, the emittance, and they are almost reversible. Second, going from a small harmonic  $h_1$  to a larger  $h_2$  requires a reduced voltage during the munch, whereas going the other way requires an increased voltage. Third, the beam distribution must stay well inside the stable phase-space area and preferably in the linear region. This is difficult when covering large steps in the harmonics  $|h_1 - h_2| \gg 1$ . If particles end up in the non-linear region, they will develop into the spiral arms, which increase the emittance and cause the sequence to become irreversible. This implies that the phase-space area occupied by the beam, its longitudinal emittance, must be significantly smaller than the area of the stable phase-space region, also known as the bucket. Conversely, if the initial emittance is comparable to the size of the bucket, we cannot munch the bunch towards higher harmonics and shorter bunch lengths.

Nevertheless we explore a gentle path towards higher harmonics in which we always double the harmonic in the following section.

### 4.3 Harmonic-doubling cascade

Since very short bunches are of particular interest, both for plasma accelerators using protons [5] and for muon colliders [6, 7] we explore a sequence of munches that pass the beam from one RF system to one at twice the frequency and then repeat this process several times. We also assume that the voltages of all RF systems are equal to  $v = 1$ , only the harmonic  $h$  doubles from one stage to the next.

The result of this simulation, based on following 10000 particles, is shown in Figure 3. The top-left image shows the initial bunch distribution at the first harmonic, which has a rms bunch length of  $10^\circ$ , which corresponds to a FWHM



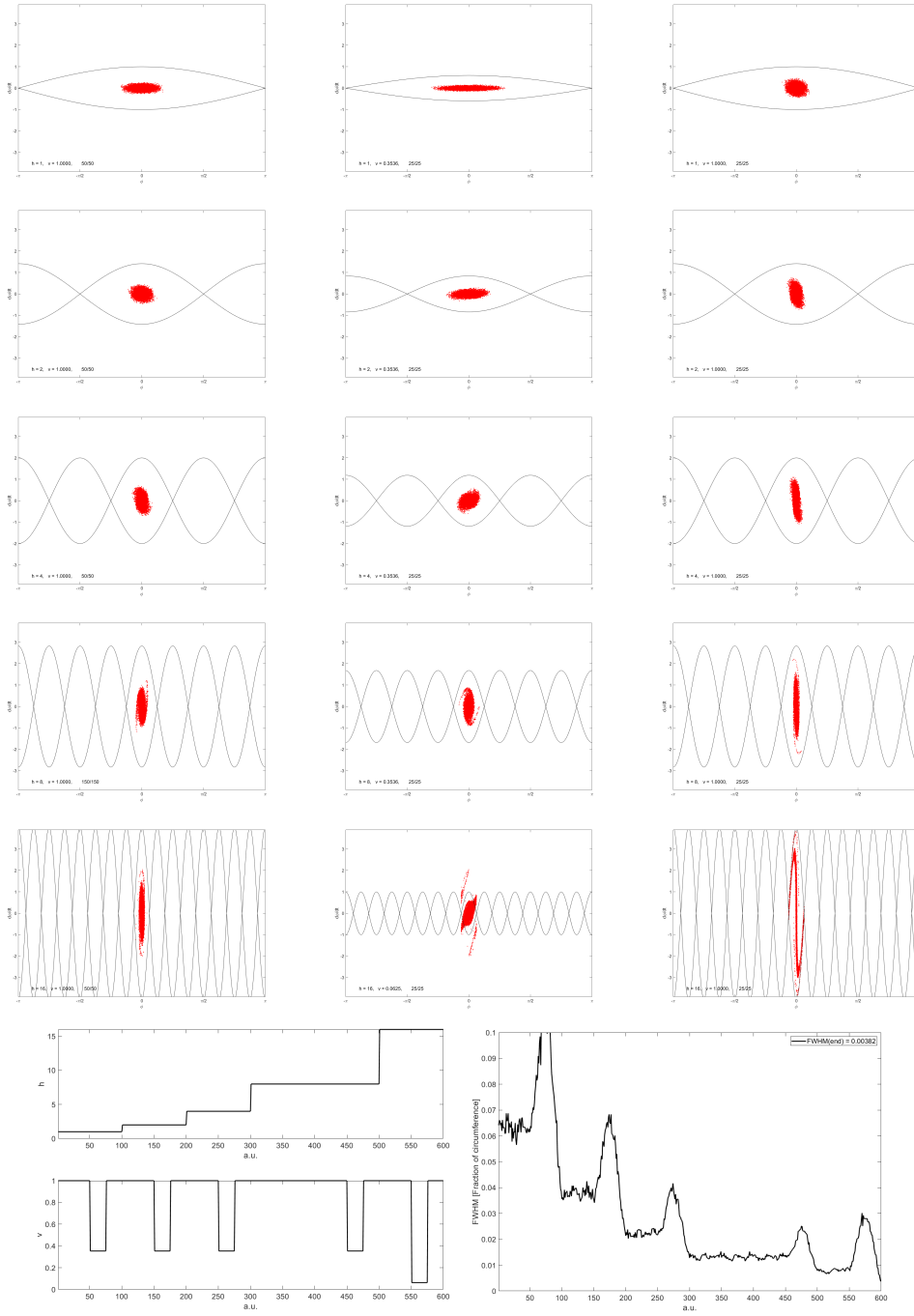


Figure 3: The phase-space distributions for the harmonic-doubling cascade. The first four rows show the bunches for the sequence harmonics  $h = 1, 2, 4, 8, 16$ , whereas the fifth row shows the final bunch to reduce the bunch length even further. The bottom row shows the evolution of harmonic (upper left) and voltage (lower left) and the evolution of the bunch length (right).

of about 6.2% of the circumference. The middle image in the top row shows the distribution after the first munch, where the voltage is dropped to  $(1/2)^{3/2} \approx 0.354$  and on the image on the right after the final quarter oscillation, at which point it is matched to the second-harmonic system. The second row shows the distribution during the time it is under the control of the second-harmonic system. The left image is taken after one half synchrotron period, the middle at the end of the munch and the image in the right after the quarter oscillation with the restored voltage to prepare a matched distribution for the fourth harmonic. Note that the height of the separatrix at the second harmonic is increased compared to the first harmonic by the ratio of the synchrotron frequencies  $\sqrt{h_2/h_1} = \sqrt{2}$ . The third row repeats the same pattern at the fourth harmonic that we switch on as the second-harmonic system is switched off. First we show the distribution after half a synchrotron period, then after the munch, and the right image shows it after the quarter oscillation with restored voltage, ready to be handed over to the eighths-harmonic system. The fourth row repeats that pattern at the eighths-harmonic to prepare the distribution for the sixteenth harmonic that is shown in the left image on the fifth row. In the middle image in the fifth row, the bunch is munched a final time with a voltage drop to  $\hat{v} = 1/9$  such that the last quarter oscillation reduces the bunch length a final time, ready to direct it onto a target. At this point it has a FWHM of about 0.004 of the circumference, which corresponds to a few ns in a 300 m ring. The two images on the bottom row of Figure 3 show the evolution of the harmonic number on the top panel of the left image and the voltage on the bottom panel. The image on the right shows the evolution of the FWHM bunch length during the process. All munches are clearly visible by the increased FWHM with subsequent drop to about 60% of the FWHM before the munch, a value consistent with Equation 8, given by  $(h_1/h_2)^{3/4} = (1/2)^{3/4} \approx 0.595$ . The FWHM after the final munch is reported in the legend.

We conclude that we can reduce the length of a bunch significantly, provided that initially it is not too large. During the transfer from one harmonic to the next, more of the stable phase space area is occupied and at some point the non-linearity of the RF voltage will prevent a transition to an even higher harmonic.

## 5 Conclusions

Within the framework of a linearized theory we derived equations to describe a bunch munch consisting of two quarter-period synchrotron oscillations at two RF voltages that transfers a longitudinally matched distribution from one RF system to another one operating at a different harmonic and a different voltage. Simulations taking the non-linearity of the RF systems into account show good agreement with the linear theory; the transferred distributions are matched and the changes of the bunch length are consistent with the linearized theory.

At the same time, simulations of the non-linear system indicate limitations of applicability. If a significant fraction of the beam distribution is located outside the linear regime near the center of the separatrix, the reversibility of the transfers is spoiled and the longitudinal emittance will grow. Moreover, if the bunch area becomes comparable to the bucket size, particles will no longer be trapped inside the same bucket and the phase space will be diluted.

We have not addressed technical aspects of implementing the bunches, though they are likely significant. Implementing the rapid changes of the RF parameter require an advanced low-level RF control system and changes of beam loading during the rapid changes pose additional problems. On the other hand, the transitions are very rapid, on the order of a few synchrotron periods, such that space-charge effects are possibly limited, though this must be investigated in detail in the future.

## References

- [1] F. Decker, T. Limberg, J. Turner, *Pre-compression of bunch length in the SLC damping rings*, SLAC-PUB-5871, presented at HEACC'92 in Hamburg, July 1992.
- [2] M. Abramowitz, I. Stegun, *Handbook of Mathematical Functions*, Dover, New York, 1972.
- [3] V. Ziemann, *Hands-On Accelerator Physics Using MATLAB*, CRC Press, Boca Raton, 2019.
- [4] MATLAB web page at <https://www.mathworks.com>
- [5] E. Adli et al., *Acceleration of electrons in the plasma wakefield of a proton bunch*, Nature 561 (2018) 363.
- [6] K. R. Long et al., *Muon colliders to expand frontiers of particle physics*, Nature Physics 17 (2021) 289.
- [7] J. P. Delahaye et al., *Muon colliders*, arXiv 1901.06150, January 2019.